INSTITUTE OF PHYSICS PUBLISHING NANOTECHNOLOGY
Nanotechnology **15** (2004) 1720–1731 PII: S0957-4484(04)83743-7

# Phase separation in nanoparticles

**A S Shirinyan**[1] **and M Wautelet**[2]

[1] Department of Physics, Cherkasy B Khmelnytsky National University, 81, Shevchenko street, Cherkasy 18017, Ukraine
[2] Experimental Photonics Group, University of Mons-Hainaut, 23, Avenue Maistriau, B-7000 Mons, Belgium

E-mail: shirinyan@phys.cdu.edu.ua and michel.wautelet@umh.ac.be

Received 14 July 2004, in final form 22 September 2004
Published 3 November 2004
Online at stacks.iop.org/Nano/15/1720
doi:10.1088/0957-4484/15/12/004

**Abstract**
The influences of the size, thermodynamic quantities and depletion of the parent phase on the separation thermodynamics of nanosized supersaturated binary solid solutions are studied theoretically. A quantitative analysis of the nucleation of one nucleus and of the decomposition in small isolated nanoparticles is presented. It is shown that three possibilities exist: phase separation, prohibition of decomposition, and formation of the metastable state of the nanoalloy. The conservation of matter leads to constraints on nucleation and growth of new phases. The case of solid–solid transition phenomena in a nanosystem is studied for regular solutions. This model leads to the existence of multiple equilibrium configurations for the same sets of initial parameters.

Phase diagrams of small particles, i.e. probability-size, nucleation barrier-solubility, temperature-composition, are plotted within a regular solution model.

## 1. Introduction

Particles with a diameter in the range of 1–100 nm are in an intermediate state between the solid state and the molecular state. When the number of atoms in the particle is in the thousand range or above, the properties evolve gradually from the molecular state to the solid state. Such particles are characterized by the fact that the ratio of the number of surface to volume atoms is not small. It is then obvious that the effects of the surface on the cohesive properties of the particle cannot be neglected. In the case of elemental particles, it is well established experimentally that, in the nanometre range, the melting temperature, $T_{\mathrm{m}}$, decreases with decreasing radius, $R$ [1]. When one extrapolates this simple argument to compound materials, one concludes that their phase diagram might differ from that of bulk material. A further argument is that segregation is known to occur at the surface of solids and liquids [2, 3].

Nanoparticles are currently the subject of much attention [4, 5]. They are of fundamental and applied interest, since they are seen in many experimental situations. They are mainly studied in the framework of solid state or technological works, like vacuum evaporation, heterogeneous catalysis, synthesis of very fine powders, nanostructures, nanoelectronics, etc. Nanoparticles are also seen embedded in structures, like so-called composite materials or clusters of implanted materials irradiated by particles arising from nuclear reactors. They would also be of interest in other fields, like astrophysics, since nanoparticles are probably present in dust in free space. When the size of particles decreases down to the nanometre range, new properties arise, due to size and quantum effects [4–9]. Recent advances in the synthesis and the characterization of size-selected particles in the nanometre range are such that it becomes possible to investigate their physical and chemical properties [10]. Despite this interest, the phase diagrams of nanostructures and their peculiarities are far from being understood.

For inorganic materials, it is known that the melting temperature, $T_{\mathrm{m}}$, decreases linearly with $R^{-1}$. This dependence is a function of the values of the surface tensions of the liquid and the crystal. Since the theoretical work of Pawlow [11] in 1909, various models have been devised to describe the variation of the melting temperature with the radius of the particle [12–17]. When the particle is not spherical (like metals embedded in polymers or other materials), it has been argued that the melting point depression might be smaller or larger than for a spherical particle, depending on its shape [18, 19]. It has also been argued that this depends on the chemical environment of the particle, via the surface tensions [20]. This has been demonstrated experimentally for the case of lead particles in pure and contaminated atmospheres [21], of In particles embedded in Al matrix [22], and others.

The phase diagram is also involved in the deposition of particles on substrates. Yeadon *et al* [23] observed the formation of heteroepitaxial interfacial layers between silver nanoparticles and a single crystal copper surface. Edelstein *et al* [24] showed that the structure and surface composition of Cu–Co nanocrystals vary.

Nanoparticles are not always uniform. In many circumstances, they consist of one core phase, surrounded by another phase, making the shell of the particle. This is the case for elemental particles surrounded by their oxide [21], metal core in another metal shell [25], etc. It is also observed that some otherwise metastable phases are stable when they are surrounded by another shell [26]. Moreover, the kinetics of the synthesis of alloys is far from being understood. In some circumstances, core–shell structures seem to appear spontaneously [25], while alloying occurs for other alloys [27].

Since very different situations exist, and due to the importance of the phase diagram in current and future applications of nanoparticles, the theoretical study of the phase diagrams of nanosystems is of great importance.

When dealing with nanoparticles, it is necessary to specify the size range under discussion. Indeed, in the literature, the term 'nanoparticle' is used for particles having sizes from a few atoms up to clusters, in the 100 nm range. The behaviour of these nanoparticles are different. When the particles contain a few hundred atoms, their shapes are often well defined polyhedra [28, and references therein]. Here, we treat cases where the thermodynamical description remains valid. This implies that:

1. the overall radius of the nanoparticle is relatively large ($R \geqslant 2$ nm) [14];
2. the radii of the core and the shell are also relatively large;
3. the surface of the core is characterized by a single value of the surface tension. This condition is met when the particle is either 'rounded' or, in contrast, presents the shape of a regular polyhedron with one kind of facet [19]. The difference between the surface tension and specific surface free energy is neglected;
4. the temperature, $T$, is an appropriate parameter to describe the 'state' of the particle. The usual definition of temperature is related to the average energy of a system of particles. This definition is for a system in equilibrium and works even for nanoscale systems [29]. It is then valid for the study of nanoparticles in thermal equilibrium.

The size-dependence of the phase diagrams has been previously studied for a few cases. Experimental results on the effect of size on phase transformations in alloys have been obtained in a few works [30]. It is shown experimentally that the 'equilibrium' phase diagram of the particle differs from that of the bulk material. In theoretical investigations based on the thermodynamical approach, the lens-shaped solidus–liquidus curves are shifted to lower temperature when $R$ decreases [9, 31–33]. A similar behaviour is expected for other phase transformations. In the following, the term 'phase diagram' refers to the size-modified one.

When the temperature is changed, phase transitions may take place. The first-order phase transformations generally start from so-called nuclei or clusters of a new phase. Nowadays techniques based on cluster nucleation and growth mechanisms are used for the production of nanocrystals, thin films, coating, nanoelectronics, quantum dots, etc [10]. Hence the nucleation theory has to be adapted to the case of nanoparticles as well [34].

In the usual treatment of nucleation, it is assumed that the reservoir of matter is very large, so that there is no problem of matter supply during nucleation. In nanosystems, such transformation should start from nucleation, but the amount of one of the elemental constituents may be not sufficient for the synthesis of the critical nucleus. In a finite system, due to the limited matter reservoir, it has been shown theoretically that the nucleation process might differ from the usual bulk case [35–38].

In previous works [39, 40], it has been assumed that the effective 'supply region' (which leads to the Gibbs free energy of a system) is described by a two-dimensional function of the concentrations in the depleted parent phase (or in the new phase) and of the new phase nucleus sizes. The present work is aimed at the study of the nucleation process, by taking into account the depletion effect. In particular, we study theoretically the mechanisms of phase separation in a solid nanosystem and describe the fundamental differences between the phase diagrams for bulk and nanomaterials, related to the non-negligible depletion of nanoparticles even at the nucleation stage.

In section 2, the basic equations for the thermodynamics of melting in small solid particles are first given. In section 3 we introduce a thermodynamic model of phase separation in nanoparticles and go over to the problem of how depletion effects can be taken into account in the case of a nanosystem. Section 4 is devoted to the analysis of the influence of size and depletion on the thermodynamics of separation and phase diagrams of regular solutions. The concluding remarks are presented in section 5. In the appendix we present the rule of parallel tangents construction for the extreme points of a phase transition.

## 2. Thermodynamic model of melting

### 2.1. Total energy of the nanoparticle

The reasoning is based on the calculation of the temperature variation of the isobaric free energy of the involved phases, $G(T)$. Let $N$ be the number of atoms in the particle. At a fixed temperature $T$, the total Gibbs free energy for a particle of $N$ atoms is given by

$$NG = NG_{\infty} + fN^{2/3}\sigma, \qquad (1)$$

where $f$ is a geometrical factor depending on the shape of the particle, $\sigma$ is the surface tension related to one atom (i.e. the surface tension divided by the number of surface atoms). The term $fN^{2/3}$ is equal to the number of surface atoms. For most inorganic materials, $\sigma$ remains nearly constant when $T$ varies [41]. $G$ and $G_{\infty}$ are the particle and the bulk energies per atom, respectively.

Let us now apply equation (1) to binary mixtures.

### 2.2. Binary mixtures

When two elements are mixed, the Gibbs free energy density (per atom) of a binary mechanical mixture is given by [42]

$$g_m = C_1h_1 + C_2h_2 - T(C_1s_1 + C_2s_2), \tag{2}$$

where $C_1$ and $C_2$ are the atomic fractions of elements 1 and 2, respectively; $h_i$ and $s_i$ are the corresponding enthalpy and entropy, respectively. The mixing causes an increase of the entropy via the configurational entropy of mixing $\Delta s_m$:

$$\Delta s_m = -k(C_1 \ln C_1 + C_2 \ln C_2). \tag{3}$$

Here $k$ is the Boltzmann constant.

If the interactions between atoms 1 and 2 are essentially the same as in the pure components, the solution is called ideal, and the Gibbs free energy density $g_{id}$ is given by

$$g_{id} = g_m - T\Delta s_m, \tag{4}$$

$$g_{id} = C_1\mu_1 + C_2\mu_2. \tag{5}$$

Hereby the chemical potentials of components $\mu_i$ ($i = 1, 2$) are

$$\mu_i = h_i - Ts_i - kT \ln C_i. \tag{6}$$

Let us further introduce the effects of the surfaces and consider the case of spherical particles. Since the configurational entropy of mixing is dictated by the overall number of atoms 1 and 2 in the system, the surface adds no term to $\Delta s_m$. Hence, only the $h_i$ are modified by the surface, via the surface tensions $\sigma_i$. If one assumes, in a first approach, that there is *no segregation*, the Gibbs free energy density of a binary particle is given by (for ideal solutions)

$$g_{part} = g_{id} + C_1g_{surf,1} + C_2g_{surf,2}, \tag{7}$$

$$g_{part} = C_1\mu_{part,1} + C_2\mu_{part,2}, \tag{8}$$

$$\mu_{part,i} = \mu_i + g_{surf,i}. \tag{9}$$

Let us assume that the total number of atoms in the particle is equal to $N$ (equation (1)). Let now $C_1 = C$ and $C_2 = (1-C)$ be the relative concentrations of atoms 1 and 2, respectively. Then

$$Ng_{part} = C(N\mu_1 + fN^{2/3}\sigma_1) + (1-C)(N\mu_2 + fN^{2/3}\sigma_2). \tag{10}$$

A little algebra leads to

$$Ng_{part} = Ng_{id} + fN^{2/3}\Gamma(C), \tag{11}$$

$$\Gamma(C) = C\sigma_1 + (1-C)\sigma_2. \tag{12}$$

These equations show that, as expected, the energy of the particle is always larger than that of the bulk material.

Let us apply the equations to inorganic materials. In these cases, it is known that the surface tensions vary only slightly with temperature, $T$. When one assumes that the $\sigma_i$ are independent of $T$, equations (11) and (12) show that, at fixed $C$, the energy of the particle is larger than that of the bulk by a quantity independent of $T$.

### 2.3. The melting criterion

Let us now look at the melting of the binary nanosystem. One has to consider the energy of the liquid phase, $G_l(T)$, relative to that of the crystalline phase, $G_s(T)$. Since, near the melting temperature $T_m$, we are well above the Debye temperature of the solid, the specific heat is approximately constant. Hence, for the elements, one has [43]

$$(G_l - G_s)_\infty = D - KT, \tag{13}$$

where $D$ and $K$ are constants for a given material. The subscript $\infty$ states that we are dealing with very large materials, i.e. with $R$ much larger than the interatomic distance. The subscripts s and l refer to the solid and liquid phases respectively. In equation (13), $(D/K)$ is the bulk melting temperature, and $D$ is the latent heat of fusion.

By taking into account the roles of the solid and the liquid phases into equation (11), one obtains the change of the Gibbs free energy (1) for a binary particle of $N$ atoms during the process of melting:

$$N(g_{part,s} - g_{part,l}) = N(g_{id,s} - g_{id,l}) + fN^{2/3}(\Gamma_s(C) - \Gamma_l(C)). \tag{14}$$

Introducing equation (13) into (14), a little algebra leads to

$$N(g_{part,l} - g_{part,s}) = N\{C(D_l - K_lT) + (1-C)(D_2 - K_2T)\} + fN^{2/3}\{C(\sigma_{1,l} - \sigma_{1,s}) + (1-C)(\sigma_{2,l} - \sigma_{2,s})\}. \tag{15}$$

$$N(g_{part,l} - g_{part,s}) = C\{N(g_{part,l} - g_{part,s})_1\} + (1-C)\{N(g_{part,l} - g_{part,s})_2\}. \tag{16}$$

This last equation is important, since it indicates that, for 'ideal solutions', the energy difference between the liquid and solid phases of a particle of binary system is the weighted average sum of the corresponding energy of the elements.

For elemental materials (as well as for a pure monatomic substance), the melting point (melting criterion) is calculated from the previous equations, by taking $N(g_{part,l} - g_{part,s}) = 0$ (and by taking $C = 0$ or 1 and $N(g_{part,l} - g_{part,s}) = 0$ for a monatomic nanoparticle). One then obtains

$$T_m = T_{m,\infty} + f(\sigma_l - \sigma_s)/(KN^{1/3}) = T_{m,\infty}\{1 - \alpha/(2R)\}, \tag{17}$$

where $T_{m,\infty}$ is the bulk melting temperature of the material. The term $(f/N^{1/3})$ is directly proportional to the ratio of surface to volume atoms. For inorganic materials, $\alpha$ is positive, between 0.4 and 3.3 nm [14].

## 3. Thermodynamic model of phase separation: solid–solid first-order phase transition

The previous reasoning is based on the assumption that there is no phase separation and segregation, i.e. the phases remain intimately mixed. In the nanoparticles, this is far from being justified. So, one has to consider the cases where phase separation takes place, like by obtaining a core–shell structure. In nanoparticles, it is also obvious that the quantity of matter is finite. Hence one has also to take into account the fact that all stoichiometries are not available, due to the above-mentioned finite quantity of matter.

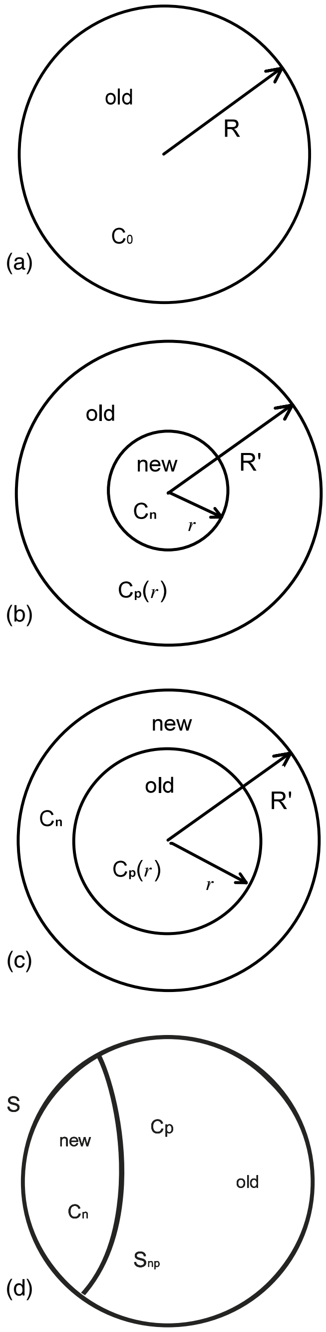

**Figure 1.** Representation of a particle of concentration $C_0$ before transformation (a) and the same particle after nucleation in different configurations of 'old' and 'new' phases ((b)–(d)): $C_p(r)$—concentration of parent phase, $C_n$—concentration of new-born phase, $r$—nucleus size (b) and radius of parent phase (c), $R$ and $R'$—radii of nanometric isolated particle before nucleation and after, respectively, $S_{np}$—surface area between the nucleus and parent phase, $S$—external surface area of new phase in the case of heterogeneous nucleation at interface boundary (d).

### *3.1. Geometry of nanoparticle and separation*

Let us assume that a small isolated initially supersaturated particle of a given alloy is quenched into the two-phase region. Then a phase transition from the single-phase state to a two-phase one takes place. A single nucleus of a new phase forms inside the particle (figure 1).

Phase separation might lead to either the formation of a core–shell structure (as studied here) or to the disintegration into two new nanoparticles. The condition to obtain the core–shell structure is that the two phases wet each other. In the following, the starting phase is called the 'parent' phase.

Let us look at the evolution of the surface energy when the core–shell structure appears. The initial surface energy of the particle is equal to

$$A_0 = 4\pi R^2 \sigma_p,$$

where $R$ is the radius of the particle before nucleation, and $\sigma_p$ is the surface tension of the free parent phase (figure 1(a)).

After nucleation, three different situations may be encountered. In the first case (see figure 1(b)), the parent phase is in the shell while the new-born phase (nucleus) is in the core of the particle. In this case, the total surface energy is given by

$$A_1 = 4\pi\{(R')^2\sigma_p + r^2\sigma_{np}\},$$

where $R'$ is the external radius of the particle, $r$ is the radius of the core material ($r \geqslant 0, r < R, r < R'$), and $\sigma_{np}$ is the specific Gibbs free energy per unit area (interphase tension) of the parent phase–nucleus interface. $R'$ may differ from $R$ when there is a difference in atomic volumes of components in the parent and new phases.

In the second case (see figure 1(c)), the parent phase is in the core while the new phase is in the shell of the particle. In this case, the total surface energy is given by

$$A_2 = 4\pi\{(R')^2\sigma_n + r^2\sigma_{np}\}.$$

Hereby $\sigma_n$ is the surface tension of the free new phase, and $r$ is the radius of the parent phase.

In the third case of heterogeneous nucleation at an external interface boundary (figure 1(d)), the two phases do not show the core–shell structure. After nucleation the corresponding value of the surface energy will be

$$A_3 = 4\pi(R')^2\sigma_p + (\sigma_n - \sigma_p)S + S_{np}\sigma_{np}.$$

$S_{np}$ is the surface area between the nucleus and the parent phase, and $S$ is the external surface area of the new phase.

When the atomic densities are the same (so that $R' = R$) the differences in surface energies between the initial single-phase state and the separated two-phase states are given by

$$\Delta A_1 = 4\pi r^2 \sigma_{np},$$

$$\Delta A_2 = 4\pi\{(\sigma_n - \sigma_p)R^2 + r^2\sigma_{np}\},$$

$$\Delta A_3 = (\sigma_n - \sigma_p)S + \sigma_{np}S_{np}.$$

When $\sigma_n = \sigma_p$, the change of surface energy may be written

$$\Delta A = \sigma_{np}S_{np},$$

where $S_{np} = 4\pi r^2$ for the cases (b) and (c) in figure 1.

The 'thermodynamic and kinetic decoding' of the transformations (a) → (c), (a) → (b), (a) → (d), (a) → (d) → (c), and so on will be more fully discussed in a future work. Here,

**Table 1.** Parameters of the binary nanosystem used in the paper.

| $Z$ | $\sigma$ (J m$^{-2}$)<br>($\sigma \equiv \sigma_{\text{np}}$) | $\varphi_{\text{AA}}, \varphi_{\text{BB}}$ (J)<br>($\varphi_{\text{BB}} = \varphi_{\text{AA}}$) | $\varphi_{\text{AB}}$ (J)<br>($\varphi_{\text{AB}} = \varphi_{\text{BA}}$) | $n$ (m$^{-3}$)<br>($n = n_1$) | $\omega_{\text{B}}$ (m$^3$)<br>($\omega_{\text{B}} = \omega_{\text{A}}$) | $R$ (m)<br>($R = R'$) | $T_{\text{c}}$ (K) |
|---|---|---|---|---|---|---|---|
| 8 | 0.15 | $-8 \times 10^{-21}$ | $-6 \times 10^{-21}$ | $7 \times 10^{28}$ | $1.43 \times 10^{-29}$ | $2 \times 10^{-8}$ | 580 |

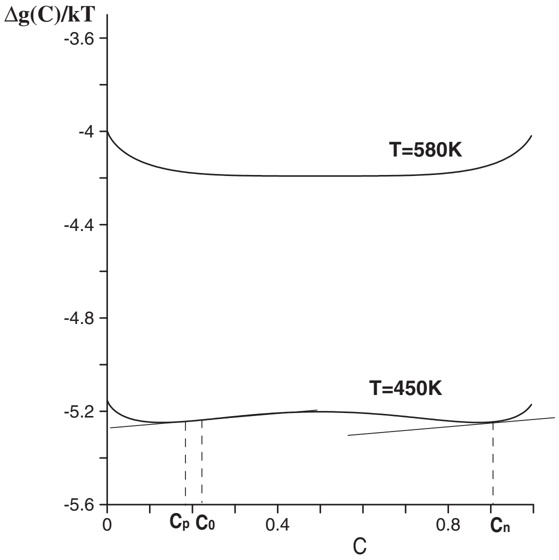

**Figure 2.** Dependences of Gibbs free energy density (per atom) on composition for different temperatures; $C_0$—initial composition. Mole fractions $C_{\text{n}}$ and $C_{\text{p}}$ are linked by the parallel tangents rule; they depend on the nucleus radius $r$ and provide the minimization of $\Delta G$ (energy of the system) with respect to concentrations for every given $r$, $R$. For the case of full decomposition in the bulk system these mole fractions $C_{\text{n}}$, $C_{\text{p}}$ tend to the values determined by the common tangent rule corresponding to stable equilibrium. Temperatures are shown in the plot. Parameters are given in table 1.

only a general thermodynamic consideration of the (a) → (b) transition is given.

In the following, we restrict the discussion to binary systems (containing A and B components) and consider the formation of a two-phase system, where the new phase has a non-zero driving force of transformation. Let us choose the thermodynamic models for the new and parent phases. The Gibbs energy (per atom) of the parent phase and of the new phase are assumed to be described by the regular solution theory (figure 2).

### 3.2. The regular solution

In the case of regular solutions, the Gibbs free energy (per atom) of formation of the new phase is given by (see, for instance [44, 45])

$$\begin{aligned}\Delta g(C) = {} & 0.5Z\{C\varphi_{\text{BB}} + (1-C)\varphi_{\text{AA}} - 2E_{\text{mix}}C(1-C)\} \\ & + kT\{C\ln C + (1-C)\ln(1-C)\} \\ & + p\{(1-C)\omega_{\text{A}} + C\omega_{\text{B}}\}. \qquad (18)\end{aligned}$$

In this equation, $\varphi_{\text{AA}}$, $\varphi_{\text{BB}}$, and $\varphi_{\text{AB}}$ are the interatomic interaction (pair) potentials between A atoms, B atoms, and A and B atoms, respectively. $E_{\text{mix}} = \{0.5(\varphi_{\text{BB}} + \varphi_{\text{AA}}) - \varphi_{\text{AB}}\}$ is the mixing energy, $Z$ is the coordination number, $p$ is the pressure, and $\omega_{\text{A}}$ and $\omega_{\text{B}}$ are the atomic volumes of A and B atoms respectively. $C$ is the relative concentration of B atoms in the system (atomic fraction of species B). Under standard conditions, ($p = 1$ atm) the last term in expression (18) may be neglected.

In the following, for simplicity, we assume that $\varphi_{\text{AA}} = \varphi_{\text{BB}}$. The parameters used in the theoretical calculations are given in table 1. We shall not discuss the results and conclusions based on the nonsymmetric approximation of the pair potentials and other values of parameters of the system since they are basically similar. The total number of atoms in the given particle is about $2 \times 10^6$, so the classical nucleation theory is appropriate.

When the stoichiometry of the new phase differs from that of the parent phase, the change of composition will lead to the depletion in the parent phase.

### 3.3. Depletion

Let us consider the binary nanoparticle to be isolated. Let us also assume that there is no constraint on lattice rearrangement. Then the process of nucleation of the new phase in the initially homogeneous system is related to the concentration fluctuations. Let $C_0$ be the mole fraction of species B in the particle before nucleation. $C_{\text{n}}$ is the mole fraction of species B in the new phase (the new phase nucleus will have another concentration than the parent phase, $C_{\text{n}} \neq C_0$), and $n$ and $n_1$ are the atomic densities in the parent and new phases, respectively.

Let us first examine the consequences of matter conservation inside the nanoparticle. The minimal volume $V^*$ of the nanoparticle for which the new phase embryo of critical volume $V_{\text{n}}^*$ can appear may be found from the conditions for matter conservation:

$$C_0 n V^* = C_{\text{n}} n_1 V_{\text{n}}^*.$$

When the embryo of the new phase appears, it requires that atoms B be taken from the parent phase. A little algebra leads to the estimation for the radius $R$ of the particle:

$$R > R^* = \left(\frac{C_{\text{n}} n_1}{C_0 n}\right)^{1/3} r_{\text{cr}},$$

where $r_{\text{cr}}$ is the radius of the critical nucleus of the new phase. The nucleation is forbidden when $R < R^*$. In the case of a system with limited volume, this condition is very important (especially for the case of large differences in compositions of the parent and new phases) even at the nucleation stage.

If the depleted parent phase is in the shell after nucleation (figure 1(b)), then the mole fractions $C_{\text{n}}$ and $C_{\text{p}}$ of species B in the new and parent phases respectively are interrelated by the formula

$$C_{\text{p}} = C_0 + \frac{n_1 r^3}{nR^3 - n_1 r^3}(C_0 - C_{\text{n}}), \qquad (19)$$

where the particle is spherical.

### 3.4. *Energy of the transition*

Under these conditions, the Gibbs free energy $\Delta G$ for the nucleation of the new phase of volume $V_\mathrm{n}$ (radius $r$) and decomposition can be written as

$$\Delta G(V_\mathrm{n}, C_\mathrm{n}) = n_1 V_\mathrm{n} \Delta g(C_\mathrm{n}) + n(V' - V_\mathrm{n})\Delta g(C_\mathrm{p}) - nV_0 \Delta g(C_0) + 4\pi r^2 \sigma, \tag{20}$$

where $\sigma$ ($\sigma_\mathrm{np}$) is the interphase tension, and $V' = V_0 + V_\mathrm{n}(n - n_1)/n$ is the volume of the separating particle after nucleation and/or separation. As pointed out previously, the change of surface energy may be written as $\Delta A = \sigma_\mathrm{np} S_\mathrm{np}$ ($S_\mathrm{np} = 4\pi r^2$). It is also assumed that the surface tension $\sigma_\mathrm{p}$ of the external surface does not change upon phase separation. Equation (20) implies that the Gibbs free energy change of the system is a function of two variables: $C_\mathrm{n}$ and $r$.

### 3.5. *Minimization procedure*

Let us now look at the equilibrium phase transformation of the nanoparticle. It is known from thermodynamics that the equilibrium is related to the concavity (or convexity) of thermodynamic potentials [44]. There are two equivalent ways to investigate this.

The first one is the usual method of geometrical thermodynamics [44, 46]. According to it, one plots the Gibbs free energy density as a function of composition, taking into account the additional surface energies related to the nucleus surface and the particle surface. Then one discusses the conditions for minimal energy of a given system.

The second way (used here) is to consider the general thermodynamic equilibrium conditions for the function $\Delta G(r, C_\mathrm{n})$ and write the equations of the first and second derivatives of $\Delta G(r, C_\mathrm{n})$ with respect to the variables.

To determine the extreme points of phase transition, one has to solve the following equations:

$$\partial \Delta G(r, C_\mathrm{n})/\partial C_\mathrm{n} = 0 \tag{21$a$}$$

$$\partial \Delta G(r, C_\mathrm{n})/\partial r = 0. \tag{21$b$}$$

The solution of the second equation of the system (21) gives the radii of the phases in the equilibrium states, at constant $T$, $C_0$ and $R$. The solution of the first one leads to the rule of parallel tangents for extreme points of transformation, at constant $r$, $R$ and $T$ (see the appendix).

The driving force for transformation is generally determined by assuming that the concentration of the parent phase is constant. As shown in the appendix, this is far from being true for nanoparticles. In the case of limited volume, one must take the depletion effect into account. The general peculiarity of nucleation is that the stoichiometry of the nucleus coincides neither with the initial stoichiometry of the parent phase nor with the stoichiometry of the new phase after transformation nor with the stoichiometry of the parent phase after separation. One usually mistakenly uses the rule of common tangent. In the appendix, a theorem for the extreme points of a phase transformation is given. According to this theorem, the optimal concentration of the parent phase after separation and the optimal concentration of the new-born phase after transformation are determined by the parallel tangents rule (not common) in the concentration dependences of the Gibbs potential density $\Delta g(C)$, when depletion of the parent phase is taken into account [39]. This is also shown in figure 2. After some algebra in the appendix the relation (A.2) obtained for the optimal concentration of the depleted parent phase and the optimal concentration of the 'new' phase is the following:

$$4E_\mathrm{mix}(C_\mathrm{n}^\mathrm{opt} - C_\mathrm{p}^\mathrm{opt}) = kT \ln \left\{ \frac{C_\mathrm{p}^\mathrm{opt}(1 - C_\mathrm{n}^\mathrm{opt})}{C_\mathrm{n}^\mathrm{opt}(1 - C_\mathrm{p}^\mathrm{opt})} \right\}. \tag{22}$$

Substituting $C_\mathrm{p}^\mathrm{opt} = C_\mathrm{p}^\mathrm{opt}(r)$ from (A.3) in this expression and solving with respect to $C_\mathrm{n}^\mathrm{opt}$, one obtains the optimal mole fraction in the new phase $C_\mathrm{n}^\mathrm{opt}$ as a function of one 'coordinate' $r$ at fixed $R$ and the other parameters of the system ($E_\mathrm{mix} < 0$). The corresponding optimal solution for the mole fraction in the parent phase $C_\mathrm{p}^\mathrm{opt}$ is determined from equation (A.3). In the following, for simplicity reasons, we write $C_\mathrm{n}$ and $C_\mathrm{p}$ instead of $C_\mathrm{n}^\mathrm{opt}$ and $C_\mathrm{p}^\mathrm{opt}$, bearing in mind the equilibrium concentrations found by the parallel tangent rule (22).

After substituting $C_\mathrm{n}$ and $C_\mathrm{p}$ into expression (20), one obtains the Gibbs free energy $\Delta G$ of the system as a function of one variable, the radius of the new phase, at constant $R$ and $T$. Equation (20) allows us to find the critical size of the nucleus and other critical parameters of the system. The condition (21$b$) for equation (20) may be rewritten as

$$n4\pi r^2\{\gamma \Delta g(C_\mathrm{n}) - \Delta g(C_\mathrm{p})\} + \frac{4\pi}{3} n((R')^3 - r^3) \left.\frac{\partial\, \Delta g(C)}{\partial C}\right|_{C_\mathrm{p}} \frac{\partial C_\mathrm{p}}{\partial r} + 8\pi r \sigma = 0.$$

Here $\sigma$ is taken independent of size $r$, and $\gamma = n_1/n$.

The last equation and the conservation of the number of atoms (19) or (A.3) determine the radius of the critical nucleus and the radius of the equilibrium (metastable or stable) two-phase configuration of the system:

$$r_0 = -\frac{2\sigma}{n\left\{\gamma \Delta g(C_\mathrm{n}) - \Delta g(C_\mathrm{p}) - (C_\mathrm{n} - C_0) \left.\frac{\partial \Delta g(C)}{\partial C}\right|_{C_\mathrm{p}} \frac{\gamma R^3}{R^3 - \gamma r_0^3}\right\}}. \tag{23}$$

In the following the atomic volumes of the constituents are assumed to be the same for the 'old' and 'new' phases ($n_1 = n$ and $\omega_\mathrm{A} = \omega_\mathrm{B}$, $\gamma = 1$).

In the general case, equation (23) is an equation of the fourth degree with respect to size $r$. Depending on the parameters the equation has either two solutions, or one solution, or has zero solution. (We neglect the $r = 0$ solution.) In the first case $\Delta G(r)$ presents one maximum (critical nucleus) and one minimum (separated two-phase state: new phase plus depleted parent phase). In the second one the maximum and minimum coincide ($\partial \Delta G(r)/\partial r = \partial^2 \Delta G(r)/\partial r^2 = 0$ for $r > 0$). In the last case, nucleation is impossible; the $\Delta G(r)$ dependence on $r$ is a monotonic increasing function.

Further, for the stability investigations of the $\Delta G(r, C_\mathrm{n})$ one must find the Jacobi determinant of the second partial derivatives of $\Delta G(r, C_\mathrm{n})$. Unfortunately, the second partial derivatives of function $\Delta G(r, C_\mathrm{n})$ with respect to $C_\mathrm{n}$ and $r$ do not give analytical solutions. So instead of this thermodynamical investigation we can:

(i) solve the conditions (21) or (22) and (23) for the equilibrium state of the system numerically and find the value of the $\Delta G$;

(ii) analyse the function $\Delta G$ (20) and evaluate the localization of extreme points of phase separation in the three-dimensional space $\Delta G$, $r$, $C_n$;

(iii) analyse only one line of the surface of the function $\Delta G$ ($\Delta G$ versus $C_n$) in three-dimensional space along the extreme path found by condition (21*a*);

(iv) analyse the summarized function $\Delta G$ (20) (as a line of the surface in three-dimensional space $\Delta G$, $r$, $C_n$) along the extreme path found by condition (21*b*).

Here, we use this last procedure.

### 3.6. *The probability factor*

The previous discussion deals with mean values of the parameters, as applied to a mean nanoparticle. Under experimental conditions, one generally deals with a large number of particles, so that a statistical approach of phase diagrams is required. The nucleation process is also inherently statistical. The crossover of the nucleation barrier is a stochastic process, which can be treated by considering the fluctuations in the system. It is therefore mandatory to study the phase separation of nanoparticles by a statistical approach.

Under equilibrium conditions, the probability of concentration fluctuation is given by the theory of thermodynamic fluctuations. The probability factor $f(r)$ is given by the Boltzmann formalism:

$$f(r) = f_0 \exp\left(\frac{-\Delta G(r)}{kT}\right) = \frac{1}{\sum_{r=0}^{r=r_{\max}} \exp\left(\frac{-\Delta G(r)}{kT}\right)} \exp\left(\frac{-\Delta G(r)}{kT}\right). \tag{24}$$

Here $f(r)/f_0$ is the fluctuation probability function for particles made of nuclei of size $r$, $1/f_0$ is the statistical sum, and $r_{\max}$ is the maximal possible size of the nucleus when the parent phase is fully depleted by species B: $C_p = 0$.

Let us recall that $\Delta G(r)$ and $f(r)$ are functions of $T$, $R$ and $C_0$. In the following, we consider the influences on the energy barriers, fluctuation probability and phase transformation of:

(i) changes of temperature $T$ at fixed other parameters;
(ii) changes of sizes $R$ at fixed other parameters;
(iii) changes of initial composition $C_0$ at fixed other parameters.

## 4. Phase diagrams: separation.

### 4.1. *Varying T*

Let us look at the variations of $f(r)$ and $\Delta G(r)$ with $T$, at fixed $C_0$, $R$ and other parameters (table 1). Typical temperature-dependent equilibrium fluctuation probabilities $f(r)$ with sizes $r$ and Gibbs free energy dependence $\Delta G(r)$ on sizes $r$ are shown in figure 3 for given sets of the parameters (hereby the rule of parallel tangents is used).

Let us start from the single-phase state at high $T$ (figure 1(a)) and let $T$ decrease. During the decrease of $T$, the dependences of $\Delta G(r)$ and $f(r)/f_0$ on $r$ change from the monotonic curves (curves 1 in figure 3) to the nonmonotonic curves with one minimum and one maximum for $r > 0$ (curves 3–5 in figure 3). One can visually compare $\Delta G(r)$ and $f(r)/f_0$. The analysis shows that the minimum of $f(r)/f_0$ corresponds to the maximum—nucleation barrier—of $\Delta G(r)$ (at the so-called critical size of the nucleus). Also, the maximum of $f(r)/f_0$ corresponds to the minimum of $\Delta G(r)$. As usual, the maximum of $f(r)/f_0$ (minimum of $\Delta G(r)$) corresponds to the two-phase equilibrium state, that is to the overcritical nucleus of the new phase and ambient parent phase (figure 1(b)). When $T$ decreases, the minimum of $f(r)$ shifts down and to the left, while the maximum moves to the right and up (figure 3(b)).

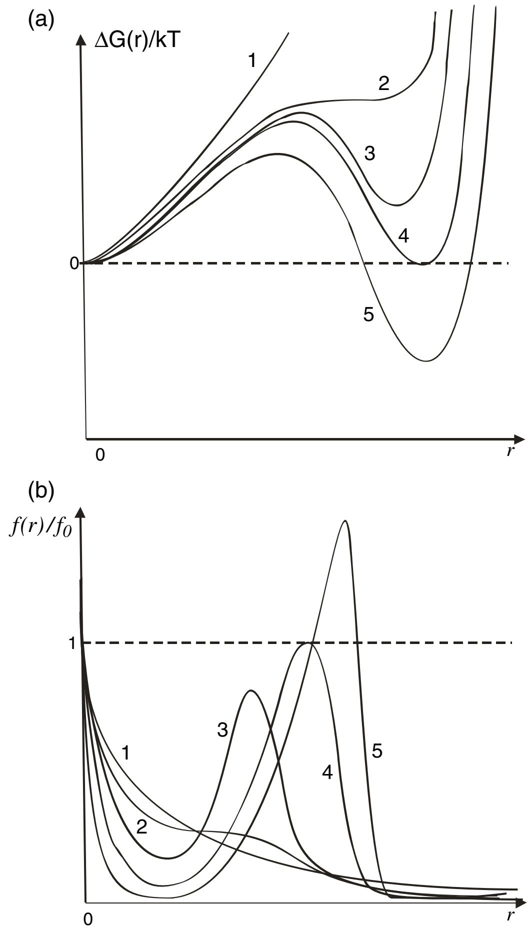

**Figure 3.** Qualitative dependence of the Gibbs free energy $\Delta G(r)$ on size (a) and fluctuation probability $f(r)/f_0$ on the radius $r$ of the nucleus (b): (i) for different temperatures $T$, provided other parameters are fixed, (ii) for different sizes $R$ and fixed other parameters, (iii) for different initial compositions $C_0$ at fixed other parameters. Explanation is presented in the main text. Case 4 represents the separation condition.

*Separation criterion.* Of particular importance is the situation where $f(r)/f_0 = 1$ (case 4, figure 3). This corresponds to the separation limit, at the separation temperature $T_{\mathrm{tr}}$. At $T_{\mathrm{tr}}$, $f(r)/f_0 = 1$, while $\partial f(r)/\partial r = 0$, $\partial^2 f(r)/\partial r^2 < 0, r > 0$. (According to formula (24) the value of $f(r)$ must be smaller than unity, but the ratio $f(r)/f_0$, which is equal to $f(r)/f_0 = \exp(\frac{-\Delta G(r)}{kT})$, may be larger than 1.) This criterion will be called the separation criterion in the following. This criterion coincides with the transition condition $\Delta G(r) = 0$, $\partial \Delta G(r)/\partial r = 0$, $\partial^2 \Delta G(r)/\partial r^2 > 0$ proposed earlier [47].

The value of $T_{\rm tr}$ depends on the value of $R$ of the particles at fixed other parameters. In principle, depending on sizes and composition, the transition temperature may vary from a few to hundreds of kelvins.

The analysis of the distribution profile (24) and formula (20) indicates the existence of three characteristic facts: single-phase states (curves 1 in figure 3); two-phase states of a nanoparticle (minimum point on curve 5 in figure 3(a) and/or maximum point on curve 5 in figure 3(b)), metastable states (minimum point for $r > 0$ on curve 3 in figure 3(a) and/or maximum point on curve 3 in figure 3(b)).

If one starts from a two-phase state at low $T$ (figure 1(b)) and increases $T$, the behaviour is the opposite. During the increase of $T$, the maximum of the $f(r)/f_0$ curve moves to the left and down and the minimum moves to the right and up (figure 3(b)). At the cross-point the maximum and minimum coincide. (For example, for $C_0 = 0.15$ and the above chosen set of parameters the condition $\partial f(r)/\partial r = \partial^2 f(r)/\partial r^2 = 0$ or $\partial \Delta G(r)/\partial r = \partial^2 \Delta G(r)/\partial r^2 = 0$ for $r > 0$ takes place at $T = 480$ K.)

The general conclusion of the present model (see, for instance, [47]) is that $T_{\rm tr}$ is a function of $R$ and initial compositions $C_0$, and that it is always smaller than for bulk material. In other words, the limited volume of the particle constrains the fluctuations in the particle so that it allows one to keep the alloy in the particle in a state which would be unstable in the bulk.

Furthermore, one can obtain all possible states by changing not only the temperature of the particle (at fixed other parameters) but also by changing the size $R$ of the particle (at fixed other parameters) as well as by changing the initial composition $C_0$ (at fixed other parameters).

### 4.2. Varying *R*

Let us now look at the influence of $R$ on the solubility at fixed $T$, $C_0$ and other parameters. As $R$ increases, the maximum of the fluctuation probability (24) appears and shifts towards the right and up, and the minimum of $f(r)$ shifts down and to the left (figure 3(b)). By means of the same reasoning as above, one deduces the existence of a separation transition criterion at a critical size of the nanosystem $R_{\rm tr}$. This value $R_{\rm tr}$ is a function of the degree of supersaturation (temperature and initial composition).

### 4.3. Varying $C_0$

Let us again fix all parameters of the system and consider the changes of initial composition $C_0$ at fixed $T$ and $R$. To investigate this one should make the previously mentioned thermodynamic analysis using the separation criterion for a small particle. As pointed out previously, this is qualitatively similar to the results of temperature or size changes discussed earlier. As the supersaturation $C_0$ becomes bigger the fluctuation probability (24) has a maximum which displaces towards big sizes (figure 3(b)). Furthermore, one can find a very interesting peculiarity, namely the existence of 'critical supersaturation' shown below.

Let us now compare the size-dependent phase diagram with that of bulk material.

### 4.4. Phase diagram

*Solubility limits in bulk material.* As a first step, we will look at the equilibrium compositions in the parent phase $C_{\rm p,\infty} \equiv C_{\rm p}(R \to \infty)$ and in the new phase $C_{\rm n,\infty} \equiv C_{\rm n}(R \to \infty)$, corresponding to the full separation in the infinite bulk material (at every fixed temperature $T$). The conditions for optimal concentration $C_{\rm n,\infty}$ and $C_{\rm p,\infty}$ and solubility limits can be found according to the common tangent rule:

$$\Delta g(C_{\rm p,\infty}) + \left.\frac{\partial \Delta g(C)}{\partial C}\right|_{C_{\rm p,\infty}} (C_{\rm n,\infty} - C_{\rm p,\infty}) = \Delta g(C_{\rm n,\infty}).$$

In the symmetric case ($\varphi_{\rm BB} = \varphi_{\rm AA}$, $\omega_{\rm A} = \omega_{\rm B}$):

$$\left.\frac{\partial \Delta g(C)}{\partial C}\right|_{C_{\rm p,\infty}} = \left.\frac{\partial \Delta g(C)}{\partial C}\right|_{C_{\rm n,\infty}} = 0,$$
$$\Delta g(C_{\rm p,\infty}) = \Delta g(C_{\rm n,\infty}).$$

This leads to the transcendental equation

$$Z E_{\rm mix}(2C_{\rm p,\infty} - 1) + kT \ln \frac{C_{\rm p,\infty}}{(1 - C_{\rm p,\infty})} = 0$$
$$\text{and} \qquad C_{\rm n,\infty} = 1 - C_{\rm p,\infty}.$$

For our set of parameters (table 1), this transcendental equation has temperature-dependent roots, $C_{\rm p,\infty}$ and $C_{\rm n,\infty}$. For regular solutions, the critical temperature, $T_{\rm c}$, at which the separation is impossible in bulk material corresponds to the conditions

$$\partial \Delta g(C)/\partial C = \partial^2 \Delta g(C)/\partial C^2 = 0,$$

$$C_{\rm n,\infty} = C_{\rm p,\infty} = 0.5.$$

In our case, $T_{\rm c} = 580$ K. The usual cupola-shaped separation diagram $T$–$C$ for an infinite matrix is given in figure 4.

Let us recall that the usual cupola-shaped equilibrium diagram determines the solubility as well as the equilibrium compositions ($C_{\rm p,\infty}$ and $C_{\rm n,\infty}$), as a result of separation by one line. In fact, in bulk material, the solubility is equal to the equilibrium composition $C_{\rm p,\infty}$. In the following, we will see that, in nanosystems, the solubility does not coincide with the equilibrium composition after separation. Moreover, one needs to re-interpret the size-dependent separation diagram for small particles.

*Size-dependent diagram.* Let us now study phase transitions in our binary nanosystem. Let us fix $R$ and $C_0$, and let us vary $T$ until $T_{\rm tr}$ is reached. Then we change only the initial composition $C_0$ at fixed $R$ and again find the new transition temperature $T_{\rm tr}$ (hereby the rule of parallel tangents is used). The conclusion of such a procedure is as follows.

According to the rule of parallel tangent construction and our separation criterion for a small particle (case 4 in figure 3) one can find the optimal composition $C_{\rm p}$ ($C_{\rm p} \equiv C_{\rm p}(R, T)$) of the parent phase corresponding to the two-phase state condition $f(r)/f_0 = 1$ (or stable $\Delta G(r)$ minimum). Thus, we have three limiting points for the chosen criterion:

(1) the initial composition as the limit of solubility $C_0^*(R, T)$ (further $C_0^*$) of one component in another (B in A);

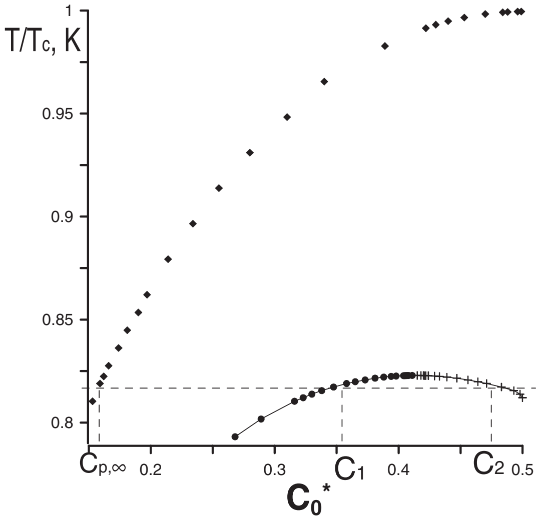

**Figure 4.** Size-dependent state diagram: reduced temperature $(T/T_c)$—solubility $C_0^*$. Points '◆' show the usual cupola-shaped diagram of a binary system for the case of separation in an infinite system (when $C_0^* = C_{p,\infty}$). Points '●' represent the first stable solution of equation (21*b*) or (23) and indicate the cupola-shaped diagram of a small particle at fixed radius $R$ (the line connecting the experimental points is plotted for visualization of the cupola shape). Points '+' correspond to the second stable solution of the system of equations (21) and continue the size-dependent phase diagram in the high-temperature range. The parameters are in table 1. Compositions $C_p$ and $C_n$ after separation are not presented in the figure.

(2) the optimal composition of the depleted ambient parent phase $C_p$ after separation;
(3) the optimal composition of the new-born phase $C_n$ as the result of separation.

Let us note that the separation criterion in the regular solution leads to an unexpected result, namely multiple values for the solubility $C_0^*$ (and respectively multiple equilibrium configurations of the system (figure 1(b))) at the same sets of initial parameters. So for simplicity we restrict the comparison with the bulk case within the concentration limits $0 < C_0 < 0.5$ (figure 4).

Let us consider the influence of finite sizes $R$ on the solubility $C_0^*$ change at fixed temperature $T$ (say, $T/T_c = 0.817$) and cited above parameters (table 1). The solubility $C_0^*$ in massive alloy is determined by point $C_{p,\infty} = 6.4$ at.% in figure 4. In the nanoparticle, we calculate $C_1 = 35$ at.%. ($C_{01}^* \equiv C_1 > C_{p,\infty}$) and $C_2 = 48.3$ at.% ($C_{02}^* \equiv C_2$—the result of the existence of the second solution of equations (21)–(23), second critical solubility). This means that a massive alloy with $C_0 < C_{p,\infty}$ is thermodynamically stable with respect to separation. For chosen temperature $T/T_c = 0.817$ in the $C_{p,\infty} < C_0 < 0.5$ interval the massive alloy is unstable, and it will be separated into a new phase of composition $C_{n,\infty} = 1 - C_{p,\infty} = 95.6$ at.% and a parent phase of composition $C_{p,\infty} = 6.4$ at.%. At the same time, a small particle with the same initial concentration $C_0$ ($C_0 < C_1$ and $C_0 > C_2$) will not be separated, but a particle with composition $C_1 < C_0 < C_2$ will be separated into a new phase and parent phase. Hence, the decrease of the size of a system leads to the increase of the solubility $C_0^*$ (figure 4).

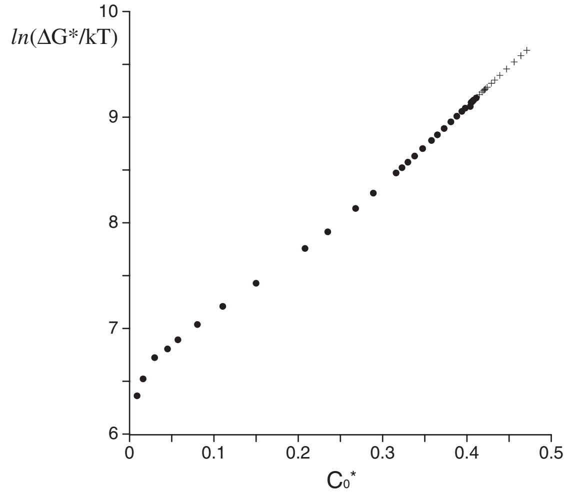

**Figure 5.** Nucleation barrier (in reduced units) in separating a particle of size $R$ as a function of solubility in the frame of a regular solution model. Points '●' and '+' indicate nucleation barriers in the case of the first and the second stable solution of equations (21), respectively. The linear approximation for solubility limits in the case of the chosen set of parameters may be written as $C_0^* \approx \{\ln(\Delta G^*/kT) - 6.15\}/7.4$.

Figure 4 shows that:

(i) spinodal decomposition in the small particle is impossible, even if we take a nanosystem at composition within the interval $\partial^2 \Delta g(C)/\partial C^2 < 0$.
(ii) there exist two stable solutions of the system of equations (21) or (22) and (23) for high temperatures in regular solutions (two pairs of $C_p$, $C_n$ and corresponding values $r$).

More careful consideration of the nucleation barriers for these two solutions leads to the result shown in figure 5.

Comparing figures 4 and 5, one can see that the second solutions (points '+' nearly $C_0^* \approx 0.5$) have much higher nucleation barriers $\Delta G^*(r)$ than the first ones (points '●').

In the framework of the classical theory of nucleation, the nucleation rate is proportional to the probability factor $f(r)$ and is given by [45]

$$J = J_0 \exp\{-\Delta G^*/kT\} \exp\{-\Delta G_D/kT\}. \qquad (25)$$

Here $J$ is the steady-state rate of formation of the 'new' phase (thermodynamically stable with respect to the initial state), $J_0$ is a frequency constant, $\Delta G^*$ is the nucleation barrier, and $\Delta G_D$ is the activation energy for diffusion across the parent phase–nucleus interface.

Let $\Delta G_1^*$ be the nucleation barrier corresponding to the separation criterion at solubility $C_1$ (first solution $C_1 \equiv C_{01}^*$), and $\Delta G_2^*$ be that concerning the case $C_2$ (second solution $C_2 \equiv C_{02}^*$) at the same parameters (table 1).

According to (25) the process is controlled by both the thermodynamic and the kinetic energy barriers of nucleation. Assuming that $\Delta G_D$ is constant, $\Delta G_1^* \ll \Delta G_2^*$ implies that $J_1 \gg J_2$.

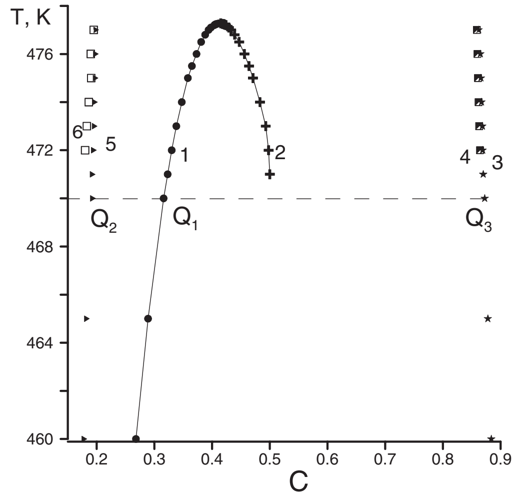

**Figure 6.** Representation of 'critical supersaturation' on the size-dependent temperature–concentration diagram of a small particle at fixed radius $R$. The parameters and explanation are presented in the main text. Results pointed by 1 and 2 are also shown in figure 4. Point $Q_1$ indicates the initial composition $C_0^*$ before nucleation, point $Q_2$ characterizes equilibrium composition $C_\mathrm{p}$ after separation, and $Q_3$ shows the optimal mole fraction in the new phase $C_\mathrm{n}$. $Q_1Q_2 \equiv \Delta C^* \equiv C_0^* - C_\mathrm{p}$—critical supersaturation.

*Critical supersaturation.* It appears from our analysis that the limiting solubility $C_0^*$ in a small particle does not coincide with the equilibrium composition $C_\mathrm{p}$ after separation. This difference between the limiting mean mole fraction of component B in initially saturated alloy (or solubility, i.e. concentration corresponding to the separation criterion) and optimal (or equilibrium) concentration in the parent phase *after* separation was earlier called a 'critical supersaturation' [47]. Hereby the difference $\Delta C^* = C_0^* - C_\mathrm{p}$ is the 'critical supersaturation'. The effect of 'critical supersaturation' means that separation is possible only (at some fixed temperature and size) if the supersaturation $\Delta C = C_0 - C_\mathrm{p}$ is larger than $\Delta C^*$. If the supersaturation $\Delta C < \Delta C^*$, then nucleation and separation are impossible. The effect of supersaturation is presented in the state diagram (figures 4 and 6).

As one can see from figure 6, two solutions exist. The first solution of the separation criterion is indicated by the set of points '●' (shown by 1) for concentrations $C_1$; points '★' (set of points shown by 3) are for the optimal concentrations $C_{\mathrm{n}1}$; and points '▶' (set 5) are for optimal values $C_{\mathrm{p}_1}$. The second solution of the separation criterion appears only at high temperatures and is shown by the set of points '+' (set 2) for the concentrations $C_2$; points '◩' (set 4) are for optimal concentrations $C_{\mathrm{n}2}$; and points '□' (set 6) are for the optimal values $C_{\mathrm{p}_2}$.

It turns out from the present analysis and figure 6 that points $Q_1$, $Q_2$, $Q_3$ correspond to the lever rule for mass conservation: $(N_\mathrm{tot} - N_\mathrm{n})\Delta C^* = N_\mathrm{n}(C_\mathrm{n} - C_0^*)$, where $N_\mathrm{n}$ is the total number of atoms in the new phase and $N_\mathrm{tot}$ is the total number of atoms in the binary system; interval $Q_1Q_2$ corresponds to critical supersaturation $\Delta C^*$.

## 5. Concluding remarks

The aim of the present work is to apply the concepts of thermodynamics to nanosystems, in the case of phase transitions.

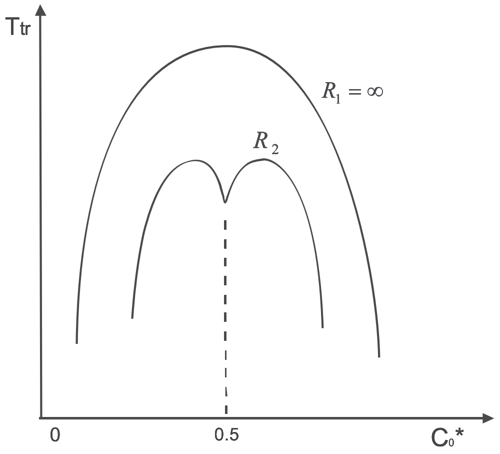

**Figure 7.** Schematic shift of phase diagram for the case of the regular solution model. The line $R_1 = \infty$ is the usual separation cupola for bulk material. The inverted W-shape dependence indicates the size-dependent diagram ($R_2 < R_1$). Compositions in the nucleus and in the parent phase after the separation of the nanosystem are not presented here.

The thermodynamic approach of the size-dependent melting temperature outlined here seems to provide a physically acceptable explanation of the melting phenomenon.

It is shown that the concept of an equilibrium phase diagram has to be revised, due to the fact that the amount of matter is limited in nanoparticles.

When a nanoparticle separates into two different phases, the equilibrium phase diagram is split and shifted, as compared with that of the bulk material. It is also size dependent. Qualitatively the shift of the phase diagram of regular solutions is as shown in figure 7.

Furthermore, instead of one line, one obtains three lines, namely a line of solubility $C_0^*$ and lines of separation $C_\mathrm{p}$ and $C_\mathrm{n}$. For example, figure 7 indicates only the solubility limits but not an equilibrium state in a nanosystem. The solubility and equilibrium compositions after separation in bulk materials coincide (case $R_1$ in figure 7).

In the case of a nanosystem, the composition limits of the new and old phases are determined by the points at which the slopes of the two free energy density curves are equal, that is have equal (not common) tangents.

Finally, we would like to point out that the investigations presented in sections 3 and 4 of the present paper are devoted to the problem of a solid–solid first-order phase transition in nanovolumes. The problem of solid–liquid transitions, based on the similar thermodynamic method, will be discussed in a forthcoming publication.

## Acknowledgments

This work is supported by the International Association for Promotion of Cooperation with Scientists from New Independent States of the former Soviet Union (Young NIS Scientist Fellowships Programme 2003, Intas Ref. Nr: 03-55-1169) and partially by the Ministry of Education and Science of Ukraine.

## Appendix. The rule of parallel tangent construction for optimal points of a phase transition

Here we demonstrate the rule which states that in the case of a nanosystem the boundaries of the phases are determined by the points at which the slopes of the two free energy density curves are equal, that is have equal (not common) tangents.

**Theorem.** *The equilibrium concentrations* $C_\mathrm{n}^\mathrm{opt}$ *in the new phase and in the ambient parent phase* $C_\mathrm{p}^\mathrm{opt}$ *are determined by the rule of parallel (not common) tangents drawn from lines of concentration dependences of Gibbs free energy densities on concentrations for the 'new' and 'old' phases.*

**Proof.** Let us find the equilibrium concentrations for problem (18)–(20). Considering the possible set of concentrations $C_\mathrm{n}$ in the nucleus, let us find the optimal one from the condition (21*a*).

According to equation (19) one should find the concentration in the parent phase $C_\mathrm{p}$ as a function of the concentration $C_\mathrm{n}$ and the volume $V_\mathrm{n}$ at other fixed parameters. Analysing equation (20), with regard to condition (21*a*), one easily obtains the relation

$$n_1 V_\mathrm{n} \left.\frac{\partial \Delta g(C)}{\partial C}\right|_{C=C_\mathrm{n}} = -n(V' - V_\mathrm{n}) \left.\frac{\partial \Delta g(C)}{\partial C}\right|_{C=C_\mathrm{p}} \frac{\partial C_\mathrm{p}}{\partial C_\mathrm{n}}. \tag{A.1}$$

Applying relation (19), one obtains

$$\frac{\partial C_\mathrm{p}}{\partial C_\mathrm{n}} = -\frac{n_1 V_\mathrm{n}}{n V_0 - n_1 V_\mathrm{n}} = -\frac{n_1 V_\mathrm{n}}{n(V' - V_\mathrm{n})}.$$

Substituting the last equation into (A.1), one obtains the rule of parallel tangent construction for optimal concentrations in the 'new' phase and in the 'old' parent phase (see also figure 2), which was to be proved:

$$\left.\frac{\partial \Delta g(C)}{\partial C}\right|_{C_\mathrm{n}^\mathrm{opt}} = \left.\frac{\partial \Delta g(C)}{\partial C}\right|_{C_\mathrm{p}^\mathrm{opt}}. \tag{A.2}$$

Then the expressions obtained for the optimal mole fraction in the parent phase will be

$$C_\mathrm{p}^\mathrm{opt} = \frac{C_0 n V - C_\mathrm{n}^\mathrm{opt} n_1 V_\mathrm{n}}{nV - n_1 V_\mathrm{n}} \quad \text{or} \quad C_\mathrm{p}^\mathrm{opt} = C_0 + \frac{n_1 r^3}{nR^3 - n_1 r^3}(C_0 - C_\mathrm{n}^\mathrm{opt}(r|R)). \tag{A.3}$$

□

**Resumé.** *The rule of parallel tangent gives the optimal path of evolution of a system. This rule is a sequence of the thermodynamic approach when the Gibbs free energy (20) is minimized:* $\partial \Delta G / \partial C_\mathrm{n} = 0$ *(21a). Solving this variation problem, an optimal depletion for fixed nucleus size is obtained, provided by the condition* $\partial^2 \Delta G / \partial C_\mathrm{n}^2 > 0$.

This rule is valid for the critical nucleus as well as for the equilibrium two-phase state (the supercritical nucleus of optimal concentration and separated parent phase being in the state of minimum of Gibbs free energy) because it is determined from the extreme condition for the Gibbs free energy change of the system.

One can show that in the extreme case of separation (not nucleation) in the infinite matrix the equal tangents become common and the driving force will be determined by the well known rule of common tangent.

In the limiting case ($R \to \infty$) the rule of parallel tangents allows us to find the concentrations in the critical nucleus and matrix correspondingly at once on the phase diagram $\Delta g(C) - C$. Hereby the composition of the parent phase stays unchanged at $C_0$.

In the general case before drawing the parallel tangents for the critical nucleus and matrix or for the equilibrium two-phase state ('new' phase plus parent phase) on the diagram $\Delta g(C) - C$ one must solve equation (21*b*) at first and then solve equation (21*a*) or (A.2).

Furthermore, the rule may be applied in a multicomponent system as well, when a new phase is not determined by strong stoichiometric composition, that is, there exists a solubility interval on the diagram of Gibbs free energy density versus concentration ($\Delta g(C) - C$).

As was mentioned before, this rule is applied for the nucleation and separation of nanoparticles in which the composition of the new phase is a function of size.

## References

[1] Buffat Ph and Borel J-P 1976 *Phys. Rev.* A **13** 2287

[2] Turnbull D 1956 *Solid State Phys.* **3** 225

[3] Sparnaay M J 1984 *Surf. Sci. Rep.* **4** 101

[4] Timp G (ed) 1999 *Nanotechnology* (New York: Springer)

[5] Wautelet M (ed) 2003 *Les Nanotechnologies* (Paris: Dunod)

[6] Petrov Y I 1982 *Physics of Small Particles* (Moscow: Science)

[7] Robbins M O, Grest G S and Kremer K 1990 *Phys. Rev.* B **42** 5579

[8] Nagaev E L 1992 *Usp. Fiz. Nauk* **162** 50

[9] Liang L H, Liu D and Jiang Q 2003 *Nanotechnology* **14** 438

[10] Bhushan B (ed) 2004 *Springer Handbook of Nanotechnology* (Berlin: Springer)

[11] Pawlow P 1909 *Z. Phys. Chem.* **65** 1

[12] Couchman P R and Ryan C L 1978 *Phil. Mag.* A **37** 369

[13] Hoshino K and Shimanura S 1979 *Phil. Mag.* A **40** 137

[14] Wautelet M 1991 *J. Phys. D: Appl. Phys.* **24** 343

[15] Vanfleet R R and Mochel J M 1995 *Surf. Sci.* **341** 40

[16] Nanda K K, Sahu S N and Behera S N 2002 *Phys. Rev.* A **66** 013208

[17] Sun C Q, Tay B K, Zeng X T, Li S, Chen T P, Zhou J I, Bai H L and Jiang E Y 2002 *J. Phys.: Condens. Matter* **14** 7781

[18] Wautelet M 1998 *Phys. Lett.* A **246** 341

[19] Wautelet M, Dauchot J-P and Hecq M 2003 *J. Phys.: Condens. Matter* **15** 3651

[20] Wautelet M 1992 *Nanotechnology* **3** 42

[21] Allen G L, Bayles R A, Gile W W and Jesser W A 1986 *Thin Solid Films* **144** 297

[22] Sheng H W, Xu J, Yu L G, Sun X K, Hu Z Q and Lu K 1996 *J. Mater. Res.* **11** 2841

[23] Yeadon M, Ghaly M, Yang J C, Averback R S and Gibson J M 1998 *Appl. Phys. Lett.* **73** 3208

[24] Edelstein A S, Harris V G, Rolison D R, Kurihara L, Smith D J, Perepezko J and da Silava Bassani M H 1999 *Appl. Phys. Lett.* **74** 3161

[25] Shibata T, Bunker B A, Zhang Z, Meisel D, Vandeman C F II and Gezelter J D 2002 *J. Am. Chem. Soc.* **124** 11989

[26] Ramos de Debiaggi S, Campillo J M and Caro A 1999 *J. Mater. Res.* **14** 2849
[27] Yasuda H and Mori H 1992 *Phys. Rev. Lett.* **69** 3747
[28] Yacaman M J, Ascencio J A, Liu H B and Gardea-Torresdey J 2001 *J. Vac. Sci. Technol.* B **19** 1091
[29] Cahill D G, Ford W K, Goodson K E, Mahan G D, Majumdar A, Maris H J, Merlin R and Phillpot S R 2003 *J. Appl. Phys.* **93** 793
[30] Gladgkikh M T, Chigik S P, Larin V N, Grigorijeva L K and Suhov V N 1988 *Dokl. Akad. Nauk USSR* **300** 588
[31] Wautelet M, Dauchot J P and Hecq M 2000 *Nanotechnology* **11** 6
[32] Vallée R, Wautelet M, Dauchot J-P and Hecq M 2001 *Nanotechnology* **12** 68
[33] Jesser W A, Shneck R Z and Gile W W 2004 *Phys. Rev.* B **69** 144121
[34] Hill T L 2002 *Thermodynamics of Small Systems* (Mineola, NY: Dover)
[35] Ludwig F P and Schmelzer J 1996 *J. Colloid Interface Sci.* **181** 503
[36] Rusanov A I 1967 *Phase Equilibriums and Surface Phenomena* (Leningrad: Chemistry)
[37] Ulbricht H, Schmelzer J, Mahnke R and Schweitzer F 1988 *Thermodynamics of Finite Systems and Kinetics of First-Order Phase Transitions* (Leipzig: BSB Teubner)
[38] Gusak A M and Shirinyan A S 1998 *Met. Phys. Adv. Tech.* **20** 40
[39] Shirinyan A S and Gusak A M 1999 *Ukr. Fiz. Zh.* **44** 883
[40] Shirinyan A S, Gusak A M and Desre P J 2000 *J. Metast. Nanocryst. Mater.* **7** 17
[41] Desjonquières M C and Spanjaard D 1993 *Concepts in Surface Science* (Berlin: Springer)
[42] Rosenberger F 1979 *Fundamentals of Crystal Growth* vol 1 *Macroscopic and Transport Concepts* (New York: Springer)
[43] Spaepen F and Turnbull D 1978 *Laser–Solid Interactions and Laser-processing* ed S D Ferris, H J Leamy and J M Poate (New York: AIP) p 73
[44] Christian J W 1965 *Theory of Transformation in Metals and Alloys* (New York: Pergamon)
[45] Seitz F and Turnbull D (ed) 1965 *Solid State Physics* vol 3 *Advances in Research and Applications* (New York: Academic)
[46] Seitz F 1940 *The Modern Theory of Solids* (New York: McGraw-Hill)
[47] Shirinyan A S and Gusak A M 2004 *Phil. Mag.* A **84** 579